The properties of free polymer surfaces and their influence on the glass transition temperature of thin polystyrene films

J.S. Sharp[1,2,a], J.H. Teichroeb[2], and J.A. Forrest[2,b]

[1] School of Physics and Astronomy, University of Nottingham, University Park, Nottingham, NG7 2RD, UK
[2] Department of Physics and Guelph-Waterloo Physics Institute, University of Waterloo, 200 University Avenue West, Waterloo, Ontario, N2L 3G1, Canada

Abstract. We present a detailed study of free polymer surfaces and their effects on the measured glass transition temperature (T_g) of thin polystyrene (PS) films. Direct measurements of the near-surface properties of PS films are made by monitoring the embedding of 10 and 20 nm diameter gold spheres into the surface of spin-cast PS films. At a temperature $T = 378\,\mathrm{K}(> T_g)$, the embedding of the spheres is driven by geometrical considerations arising from the wetting of the gold spheres by the PS. At temperatures below T_g ($363\,\mathrm{K} < T < 370\,\mathrm{K}$), both sets of spheres embed 3–4 nm into the PS films and stop. These studies suggest that a *liquid-like* surface layer exists in glassy PS films and also provide an estimate for the lower bound of the thickness of this layer of 3–4 nm. This qualitative idea is supported by a series of calculations based upon a previously developed theoretical model for the indentation of nanoscale spheres into linear viscoelastic materials. Comparing data with simulations shows that this surface layer has properties similar to those of a bulk sample of PS having a temperature of 374 K. Ellipsometric measurements of the T_g are also performed on thin spin-cast PS films with thicknesses in the range $8\,\mathrm{nm} < h < 290\,\mathrm{nm}$. Measurements are performed on thin PS films that have been capped by thermally evaporating 5 nm thick metal (Au and Al) capping layers on top of the polymer. The measured T_g values (as well as polymer metal interface structure) in such samples depend on the metal used as the capping layer, and cast doubt on the general validity of using evaporative deposition to cover the free surface. We also prepared films that were capped by a new non-evaporative procedure. These films were shown to have a T_g that is the same as that of bulk PS (370 ± 1 K) for all film thicknesses measured (> 7 nm). The subsequent removal of the metal layer from these films was shown to restore a thickness-dependent T_g in these samples that was essentially the same as that observed for uncapped PS films. An estimate of the thickness of the liquid-like surface layer was also extracted from the ellipsometry measurements and was found to be 5 ± 1 nm. The combined ellipsometry and embedding studies provide strong evidence for the existence of a liquid-like surface layer in thin glassy PS films. They show that the presence of the free surface is an important parameter in determining the existence of T_g reductions in thin PS films.

PACS. 64.70.Pf Glass transitions – 68.35.Ja Surface and interface dynamics and vibrations – 68.47.Mn Polymer surfaces

Introduction

The study of thin polymer films is a fascinating and active area of research. Many of the studies in this area are motivated by advances in nanotechnology and the result of such studies is the production of an increasing number of technologically important systems on ever decreasing lengthscales. To fully understand the physics of these systems, an understanding of the properties of materials at these lengthscales is required. It is certainly not obvious that the properties of such highly confined materials will be the same as those of the corresponding bulk material, or even predictable from the bulk properties. To date, a large emphasis has been placed on the investigation of anomalous properties of thin polymer films [1]. Of particular interest have been studies of the dynamics in thin polymer films, where quantities such as the glass transition temperature (T_g), chain diffusion and intrinsic viscosity have been shown to display significant deviation from bulk behaviour [2].

Perhaps the most well studied of these phenomena is the T_g of thin polymer films. Keddie, Jones and Cory made the first observation that thin PS films (< 40 nm) on Si

ᵃ e-mail: `james.sharp@nottingham.ac.uk`
ᵇ e-mail: `jforrest@uwaterloo.ca`

substrates exhibit a T_g value that is reduced below the bulk value of PS [3]. These initial observations motivated a number of other studies that attempted to characterise the T_g of thin PS films. Whilst a uniform consensus of opinion still does not exist, dilatometric measurements of the polymer PS on a variety of different substrates have shown qualitatively that the T_g value is reduced below the bulk value for films with thickness $h < 40$ nm. Similar effects have been observed in other polymers such as PMMA [4–7], but in those cases the results have shown a more pronounced sensitivity to the surface chemistry of the substrates used. One explanation proposed for the reduced T_g values reported in thin PS films is the existence of a surface layer that has an enhanced mobility relative to that of the bulk polymer. A logical extension of this idea resulted in the study of the T_g of free standing PS films [8]. These experiments revealed much larger T_g reductions than the studies of supported PS films and showed an unexpected dependence on M_w. Such a dependence on M_w was not observed in the supported film studies [9]. A detailed study of the T_g of free standing films of PS over a wide range of M_w revealed a complicated behaviour. For large molecules ($M_w \gtrsim 500000$) the T_g reductions were found to vary linearly with the thickness of the film and were also found to depend on the M_w of the polymer. These results are indicative of chain confinement effects [10] and despite some recent theoretical attempts [11] are not yet fully understood. For PS films with $M_w \lesssim 350000$ the observed behaviour was qualitatively different. It is remarkable that these low M_w free standing films exhibit film thickness dependence of the measured T_g values very similar to that of supported PS films. In fact, a more detailed comparison revealed that *the T_g value of a free standing film of thickness h is the same as that of a supported film of thickness $h/2$* [12].

A number of models have been developed in an attempt to describe the thickness dependence of the T_g in thin films. These can be grouped into those that incorporate the existence of enhanced surface dynamics [12–14] and those that do not [15,16]. The observed correspondence between the T_g's of supported and free standing films reported above suggest some degree of merit in the "layer model" approaches that have been used to try to describe the reduced T_g values. Most importantly, the correspondence between the T_g values of supported and free standing films of low M_w ($\lesssim 350000$) PS provides strong evidence that the volume fraction of the near-surface region is a key determining factor in the T_g value of thin polymer films. Developing a clear understanding of the surface properties is therefore a key step in finding the mechanism behind T_g reductions in thin polymer films.

In considering the existence of anomalous surface dynamics in polymeric materials there are two main questions to be addressed. Firstly, how do the properties of the polymer surface differ from those of the bulk polymer (if at all) when it is in the glassy state? Secondly, if the properties of the surface are not the same as the bulk polymer, how does this affect measured properties, such as the T_g of thin film samples? The first of these questions

has been the subject of a number of recent studies. Direct measurements of the free surface properties have so far proven inconclusive. Frictional force measurements suggest an enhanced surface mobility [17], but recent shear force modulation studies indicate otherwise [18]. A notable difficulty with such nano-rheological studies is that the uncertainties in the tip shape and size lead to uncertainties in the stresses applied to the sample. In addition, the tip interacts with some near-surface region, the size of which is difficult to quantify. A further complication with such studies is that they use scan rates of a few Hz and recent experiments have shown that even frequencies as high as this can supress the observed T_g reductions in thin polymer films [19]. A less intrusive approach is to apply a small perturbation to the surface, and then use imaging techniques to monitor the relaxation of the perturbation. Unfortunately, this approach has also failed to lead to a consensus of opinion. Hamdorf and Johansmann measured relaxation of micron sized surface asperities and concluded that the polymer surface remained glassy until the bulk T_g value [20]. In contrast Kerle *et al.* used nm sized asperities and showed that these surfaces displayed significant relaxation at temperatures well below the bulk T_g value of the polymer [21]. The interaction of probe particles with polymer surfaces have also been studied. Two different experiments using micron sized probes have shown that the probes adhere to the polymer surface at temperatures below the bulk T_g [22–24]. Nanometre sized particles produced by evaporative metal deposition have also been studied and this work suggests the existence of enhanced surface mobility at temperatures below the bulk T_g value of the polymer [25].

A direct way to ascertain the effects that free surfaces have upon the measured glass transition temperature is to modify the surface and study the resulting effect on T_g. The results of these studies may be used as indirect evidence for the existence, or lack thereof, of enhanced surface dynamics. The idea is that by removing the free surface any surface enhanced mobility will be removed. Given the remarkable correlation discussed above between the T_g values of supported and free standing films, we might expect that covering the remaining free surface would remove the observed thickness dependence of the T_g in thin supported polymer films. Such studies have been presented, but the results were unexpected. Measured T_g values for SiO_x coated PS films were found to be essentially the same as those for supported films with one free surface [9]. This surprising result was subsequently confirmed in dielectric studies of Al coated PS which also showed the same T_g behaviour as that of supported films [26]. The comparison between these results and the suggestion from the T_g values measured in free standing films results in an apparent and striking inconsistency. If the free surface is important in causing reduced T_g values in thin films then eliminating the free surface *must* have an influence on the measured T_g values. The fact that this does not seem to be the case has proven to be a major obstacle in understanding glass transitions in thin polymer films.

In this paper we consider the existence of a surface layer in PS films that has enhanced dynamics relative to the bulk properties. We also consider the effects that this mobile surface layer has upon the measured T_g value of thin PS films. To determine if such a layer exists we present a detailed study of the embedding of nanometer sized gold spheres for temperatures $T > T_g$ and $T < T_g$. For the case of $T > T_g$, these studies combined with detailed calculations provide a direct and quantitative measure of the viscoelastic properties of the polymer surface. For $T < T_g$, the comparison between the data and calculations allows us to draw semi-quantitative conclusions about the properties of the near-surface layer of PS films. We also examine the effects that the free surface has on the measured T_g value in an attempt to address the inconsistencies discussed above. We motivate the idea that simply coating the free surface by thermally evaporating a capping layer on top of the polymer, may not remove memory of its existence. We provide strong evidence that suggests that the evaporation process may not give rise to the intended samples because of subtle differences in the structure of the polymer-metal interfaces produced. We also describe an alternative method for producing samples with no free surfaces, that does not involve evaporating metals directly onto polymer surfaces. These non-evaporatively capped samples show bulk T_g values for all film thicknesses in the range 7 nm $< h <$ 270 nm. Finally, we use a chemical process to remove the Al capping layer and find that the resulting samples exhibit T_g reductions that are, within experimental uncertainty, the same as that of simple supported films. Detailed tests show that the chemical procedure used to remove the capping layer does not affect the T_g value of any PS films in the thickness range of interest. Together the results provide convincing evidence that there is a mobile surface layer in PS films and that the free surface is the dominating factor in determining the T_g reductions in thin polymer films.

Experimental

Embedding studies

Solutions of polystyrene (PS) ($M_n = 214000, M_w/M_n = 1.03$, Polymer Source Inc.) were prepared by dissolving the polymer in toluene. A 3 wt% solution of PS was spin coated onto 1 cm $\times$ 1 cm single crystal silicon (Si) wafers (Compart Technology, [100] orientation) using a spin speed of 1500 RPM. This resulted in PS films with a thickness of approximately 180 nm (as determined using ellipsometry). The PS films were annealed under vacuum at 403 K for 20 hours. This was done to remove residual solvent, relax the polymer chains and to relieve any residual stresses introduced into the films during spin coating. The measured T_g of the films was determined to be 370 ± 1 K. After annealing, the samples were allowed to cool to room temperature whilst still under vacuum. The PS films were then removed from the vacuum oven.

Unconjugated gold colloid suspensions with particle diameters of 10 and 20 nm were purchased from Ted Pella Inc. The concentrations of these suspensions were approximately 5.7×10^{12} and 7.0×10^{11} particles/ml, respectively. The suspensions contained 0.01% residual $HAuCl_4$ as a result of the chemical process used in producing the nanospheres. The colloidal solution was diluted 1 : 50 with de-ionized water and a drop of the resulting solution was placed on each of the PS coated Si wafers and allowed to dry for approximately two days at room temperature. The gold nanoparticles were characterized by using transmission electron microscopy (TEM) of colloid coated free standing PS films to determine the size and shape of the spheres.

Imaging of the nanoparticle coated PS films was done using a ThermoMicroscopes Explorer atomic force microscope (AFM, Veeco) in tapping mode. Tapping mode was used because the spheres were found to move when imaged using contact mode AFM. The tips used typically had a radius of curvature of 10–20 nm. As a result of the tip shape the lateral features observed in the AFM images represent a convolution of the sphere shape with that of the AFM tip. The out-of-plane features that are measured with the AFM are insensitive to the shape of the AFM tip. As a result, the distance between the top of the nanoparticles and the PS surfaces could be accurately determined. The different interactions between the tip and the gold spheres and the tip and the polystyrene surface were expected to result in different tip-sample distances for the two different materials. Such effects may introduce small errors in an absolute determination of the height, but have no effect on the *changes* in the measured height. These changes were well represented by the difference in apparent heights measured. During imaging of the nanoparticle covered surfaces, care was taken to use the same imaging parameters on all the samples studied. This ensured that the forces applied to the spheres were the same in each experiment. Preliminary imaging of the samples was performed by using an optical microscope to determine if the samples were of sufficient quality to proceed. AFM was then used to further narrow down the best imaging region to a suitable area with enough spheres to produce a good average [27,28]. The areas were chosen such that there were at least 3 sphere diameters of space in between adjacent spheres so that interaction effects between spheres could be ruled out. The time-dependent embedding studies made use of a custom built hot stage that allowed the same spot on the sample to be imaged for the entire temperature run. This stage allowed for removal of the AFM head unit during heating and subsequent replacement of the head to within approximately two microns of the original spot after the heating cycle was completed. Samples were annealed for fixed periods of time between each image. The process of removing the head, annealing, replacing the head and imaging was repeated until the total annealing time was reached. It is an important point that in between each annealing cycle the sample is held at room temperature (293 K). The fact that embedding does not seem to occur during the time the sample is imaged (or otherwise held at room temperature) means that *the polymer surface is glassy at T = 293 K*. This is important

as similar studies have indicated embedding can occur at temperatures as low as $T = 313$ K [29]. In each experiment, the same group of spheres was used in order to reduce the time required for imaging. Doing this meant that a suitable average could be achieved with around 15 spheres instead of the 40 used in previous studies [27]. All of the samples were kept at a constant temperature of 301 K during each image measurement. Image analysis was performed using ThermoMicroscopes SPMLab software and measurements of the height were taken relative to the polymer surface, within the errors introduced by the surface roughness of the glassy PS films.

Ellipsometry studies

Ellipsometric measurements of the glass transition temperature (T_g) in thin polystyrene (PS) films were performed using an Exacta 2000 nulling ellipsometer (Waterloo Digital Electronics) with a laser wavelength of 633 nm and an incident angle of $60.0 \pm 0.1°$. Polymer films were prepared by spin coating solutions of PS ($M_w = 601200$, $M_w/M_n = 1.07$, Polymer Source Inc.) in toluene onto 1.5 cm × 1.5 cm single crystal silicon substrates ([100], Compart Technology). All of the films were prepared using a spin speed of 3000 RPM. The thickness of the films was controlled by varying the concentration of the PS solutions. Film thicknesses (h), in the range from 8 nm to 290 nm were produced using this method. The PS films were then annealed under vacuum at 403 K (Bulk $T_g = 370 \pm 1$ K) for 8 hours, allowed to cool to room temperature and then placed on a Linkam hot stage and mounted onto the ellipsometer sample stage. The Linkam hot stage was used to control the temperature during the T_g measurements. The films were then heated to 403 K and allowed to thermally equilibrate. The equilibration typically took less than 1 minute. The samples were then cooled to 313 K at 1 K min^{-1} and the positions of the polariser (P) and analyser (A) required to obtain a null at the photodiode detector were recorded every 0.5 K. Plots of P and/or A *vs.* temperature where then used to determine the T_g of the polymer films. The raw P and A data obtained for uncapped PS films of thickness 8 nm (thinnest film) and 290 nm (thickest film) are shown in Figure 1. The T_g is defined as the temperature where the two linear least square fits to the regions corresponding to the expansion of the melt and glassy regions in these plots intersect. The ratio of the expansion coefficients in the melt and glassy regions was also determined by taking a ratio of the slopes of these linear constructions. For thick (> 100 nm) uncapped PS films, the value of this ratio was determined to be between 3 and 3.5. These values are consistent with bulk values of this ratio that have been reported in other studies of PS [30,31].

The process described above was repeated for PS films in the same thickness range that had been coated with a 5 nm thick, thermally evaporated layer of aluminium (Al) and for PS films coated with a 5 nm thick evaporated gold (Au) layer. Two sets of each of these metal coated samples
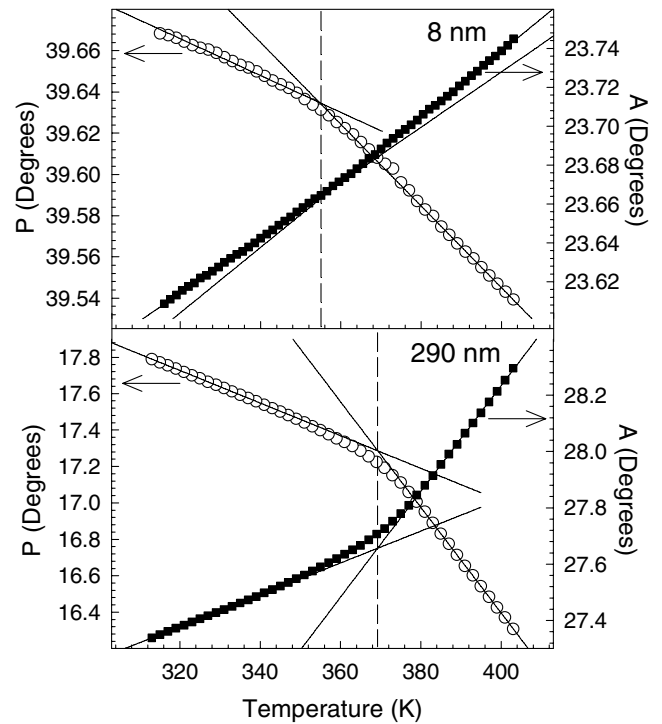
Fig. 1. Ellipsometric T_g data obtained for uncapped polystyrene (PS) films. Both P (○) and A (■) data are shown for an 8 nm thick PS film and a 290 nm thick film that were cooled from 403 K to 313 K at 1 K min^{-1}. The T_g is defined as the temperature at which the linear constructions to the regions corresponding to the expansion coefficient of the melt and the glass intersect.

were produced. In each case, the first set was annealed under vacuum at 403 K for 8 hours and allowed to cool to room temperature before the metal layer was evaporated onto the PS films. The second set of films was stored under ambient conditions for 18 hours following the spin coating procedure. They were then coated with a metal layer and annealed under vacuum at 403 K for 8 hours. These two different procedures were used to determine the effects of the evaporation/annealing history upon the T_g of metal capped PS films. The thermal evaporation of the metal capping layers was performed at an ambient pressure of 8×10^{-6} torr and the change in frequency of a 5 MHz quartz crystal oscillator mounted close to the samples in the evaporation chamber was used to measure the thickness of the metal layers. The evaporation rate used in preparing the metal capped films was 8.85×10^{-6} kg m^{-2} s^{-1}. This corresponds to growth rates of 0.5 nm s^{-1} for Au (density = 19300 kg m^{-3} [32]) and 3 nm s^{-1} for Al (density = 2700 kg m^{-3} [32]) respectively. These low evaporation rates were used so that the thickness of the metal capping layers could be reproducibly controlled. The thickness of 5 nm used was chosen so that the PS films were capped with a metal layer, but also so that sufficient optical penetration of the capping layer could be achieved to perform the ellipsometric T_g measurements. During the evaporation procedure, a copper-constantan (40 AWG, Omega) thermocouple was suspended in the evacuated

evaporation chamber so that it was close to the samples. The temperature measured by the thermocouple was typically found to be 350 K during evaporation of the metals. The temperature of the samples measured during evaporation was not found to vary significantly ($\sim$ 3–4 K) between the Al and Au evaporation procedures and this temperature was determined to be a reasonable upper bound for the temperature of the thin polymer film samples during thermal evaporation of the metals. Confirmation that continuous metal capping layers were formed during this process was obtained by collecting AFM images of the capped films before and after the samples were annealed.

The details of the interfacial structure between the polymer and the evaporated metal layer may contain information about the effect the evaporated metal layer has upon the thin film T_g values. Such information is not readily available because the PS-metal interface is buried. To study this structure of the polymer-metal interface in each case we produced a series of samples engineered to allow exposure of the normally buried interface. The samples for these experiments were prepared by thermally evaporating a thick ($\approx$ 1 μm thick) metal layer on top of a 197 nm thick spin-cast PS film, supported on a single crystal NaCl substrate. These samples were prepared using the same evaporation rates that were used for the deposition of the metal capping layers in the T_g experiments described above. Two sets of films were prepared for each metal capping layer, one set where the PS films were annealed before evaporating and the other set where the metal layer was evaporated before annealing the polymer. All of the resulting metal capped PS films were then placed face down on a clean Si substrate and the NaCl was dissolved away using deionised water. Surfaces forces pulled the metal layers into contact with the Si substrates. The PS films were then dissolved away using toluene. This resulted in an "inverted" metal surface that was a replica of the previously buried metal-PS interface. The metal surfaces were imaged using a ThermoMicroscopes Explorer AFM in contact mode. AFM images were taken using a number of different scan sizes ranging from 10 μm × 10 μm to 100 μm × 100 μm. The metal surfaces were imaged and rinsed with toluene. Subsequent imaging of the same surfaces showed that continued rinsing did not significantly alter the structures observed on the metal surfaces.

A final set of samples was prepared in an attempt to remove the effects of the free surface without the uncertainties introduced by thermally evaporating metal capping layers on top of polymer films. These samples were prepared by placing two films of similar thickness with their free surfaces in contact. One film was spin coated directly onto a 1.5 cm × 1.5 cm single crystal Si substrate ([100], Compart Technology). A second film (of similar thickness) was then spin coated from the same PS solution on to a single crystal sodium chloride (NaCl) optical window (Alfa Aesar) that had been coated with a 5 nm thick thermally evaporated Al layer (using an evaporation rate of 8.85×10^{-6} kg m^{-2} s^{-1}). The PS film supported on the Al coated NaCl was then turned upside down and placed on top of the PS film supported on the Si substrate.

A drop of deionised water (Milli-Q) was placed in contact with one edge of the NaCl substrate. This was done to partially dissolve the optical window. The water was found to preferentially wet the NaCl/Al interface and to cause the PS film and thin Al layer to debond from the NaCl window. The two PS films were then pulled into intimate contact by surface forces. The resulting $2(h/2)$ films of thickness h were rinsed in deionised water to remove any residual NaCl and then annealed under vacuum, at 403 K for 8 hours. This procedure produced samples that were identical in appearance to Al coated spin-cast PS films of similar thickness. The T_g of the $2(h/2)$ films was determined for films in the thickness range from 7 to 270 nm using the method described above. The effects of completely removing the Al capping layer from the $2(h/2)$ films were also considered. This was done by immersing the films in a 1 M NaOH$_{(aq)}$ solution for 5 minutes until the Al coating on the $2(h/2)$ films had dissolved. This concentration of NaOH$_{(aq)}$ and immersion time were determined to be sufficient to completely remove a 500 nm thick evaporated Al layer from a Si substrate. After the NaOH treatment the samples were rinsed with deionised water and the T_g values measured again. Tests indicate that this procedure has no effect on the T_g of simple supported PS films.

Results and discussion

Embedding of nanoparticles into PS films

Films with $T > T_g$

In order to use embedding studies to learn about the properties of glassy polymer films and the possible existence of a more mobile surface layer, it is first necessary to gain as much information as possible in the more simple case where $T > T_g$. It is reasonable to expect that in the case of the polymer liquid, the properties of the film are homogeneous *i.e.* the surface dynamics should be similar to those in the bulk of the liquid. This is supported by recent X-ray photon correlation studies [33] that provided evidence that in the polymer liquid, the surface has a viscosity that is the same as the bulk value. In the case of a homogenous liquid film, the spheres should embed until the angle between the flat surface and the spheres is equal to the PS/Au contact angle [27,28,34]. Figure 2a) shows a schematic diagram of this mechanism. Experimentally, this effect was manifested as a similarity between the ratio of apparent height to the initial value (sphere size) as a function of time (*i.e.* $h(t)/h_0$ was the same for the 10 nm and 20 nm spheres as $t \to \infty$).

At the lengthscales associated with the gold nanoparticles, the dominant driving force for embedding is expected to arise due to surface tension forces that act at the contact line between the particles and the PS meniscus. Assuming that the PS wets the gold particles with an angle that is equal to the equilibrium gold/PS contact angle (θ), at temperatures above T_g, then we can derive the functional form of the force acting on the particles.
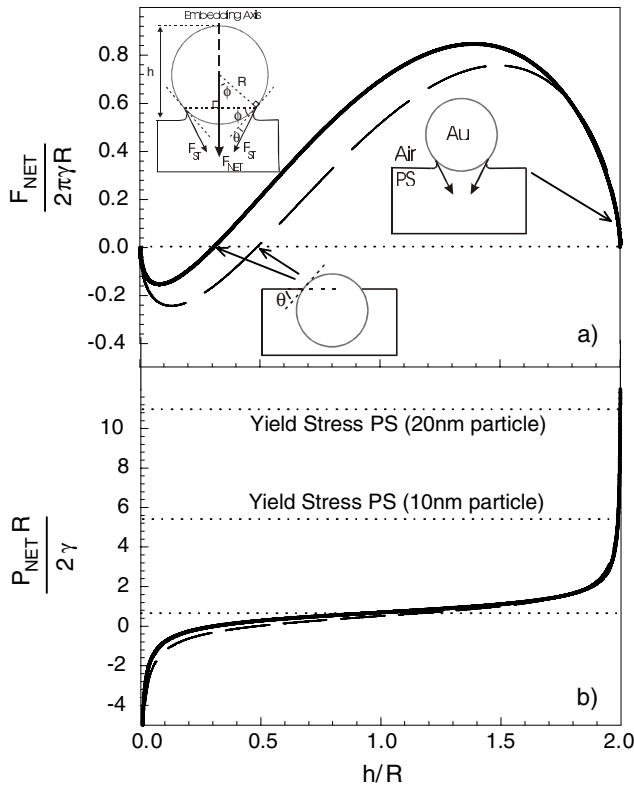
Fig. 2. Suggested mechanism for the embedding of Au spheres into polymer surfaces. Panel a) shows the magnitude of the reduced component of the surface tension force ($F_{\mathrm{NET}}/2\pi\gamma R$) exerted by the PS meniscus on the Au particles in the direction parallel to the embedding axis, as a function of the reduced embedding height, h/R. A schematic diagram showing the forces acting on the Au particles by the PS meniscus is shown in the top left of panel a). The form of the reduced force is plotted for values of the equilibrium contact angle, θ, that are equal to $46°$ (solid line) and $59°$ (dashed line). The diagrams used in panel a) show that the spheres continue to embed until the tangent to the spherical particles makes an angle with the plane of the PS surface that is equal to the equilibrium PS-Au contact angle. The force calculated in panel a) is such that a positive value represents a net *downward* force acting on the particles. Panel b) shows the variation of the reduced pressure ($P_{\mathrm{NET}}R/2\gamma$) as a function of the reduced embedding height of the particles for equilibrium PS/Au contact angles of $46°$ (solid line) and $59°$ (dashed line). The horizontal dotted lines mark the value of the reduced pressure that corresponds to the yield stress of PS (measured at 298 K) for each of the particle diameters studied [37].

This was done by resolving the components of the surface tension forces in the direction parallel to the embedding axis. The inset in Figure 2a) shows a diagram of the forces acting on the gold nanoparticles. The components of the force resolved parallel to the embedding axis give rise to a net downward force, F_{NET}, that has the same functional form as that derived by Orr *et al.* [35] for the forces exerted by the liquid bridge between a solid sphere and a liquid surface:

$$F_{\mathrm{NET}} = 2\pi R\gamma \sin(\phi)\sin(\theta + \phi) . \qquad (1)$$

In the above equation, R is the radius of the gold nanoparticle, γ is the surface tension of PS and ϕ is the angle subtended by the embedding axis and the radial line between the centre of the sphere and PS/Au contact line (as shown in the inset Fig. 2a)). From a consideration of the inset in Figure 2a) it can be shown that the angle ϕ can be related to the embedding height, h, using the approximation $\cos(\phi) \approx \frac{h-R}{R}$. In practice this may represent a rather crude approximation as it assumes that the height of the PS meniscus above the PS surface is negligible compared to the embedding height. The implications of this approximation and the effects that it has on the ability of the model to describe the embedding of the Au spheres is discussed in more detail below.

The net downward force acting on the particles can then be used to calculate the pressure exerted by the particles on the surface, P_{NET}, using the relationship $P_{\mathrm{NET}} = \frac{F_{\mathrm{NET}}}{\pi R^2 \sin^2(\phi)}$. Figures 2a) and b) show plots of the reduced force $\frac{F}{2\pi R\gamma}$ exerted on the gold particles and the reduced pressure exerted on the PS surface by the particles as a function of the reduced embedding height $\frac{h}{R}$. This was done for values of the equilibrium PS/Au contact angle of $46°$ (solid lines) and $59°$(dashed lines, see below). Figure 2a) can be used in conjunction with typical values for the temperature-dependent behaviour of the surface tension of PS [36] to show that that the forces acting on the particles due to surface tension are of the order of $\sim 1 \times 10^{-9}$ N. The force exerted by gravity on a 20 nm gold particle (assuming the density of gold to be 19300 kg m^{-3} [32]) is $\sim 8 \times 10^{-19}$ N. Forces due to gravity and hence the buoyancy of the particles can therefore be neglected. Figure 2b) shows the stresses (P_{NET}) that are exerted by the Au particles on the PS surface and shows that P_{NET} is smaller than the yield stress of polystyrene (88.5 MPa, as measured at ~ 298 K [37] and denoted by the horizontal dotted lines in Fig. 2b)) for all embedding heights smaller than $1.98R$. This corresponds to embedding distances of less than 0.2 nm for both the 10 nm and 20 nm Au particles. The plots in Figure 2b) therefore show that non-linear viscoelastic effects are not exected to play a significant role in determining the embedding behaviour of the particles into the PS once they have embedded by more than 0.2 nm.

Figure 3 shows a more detailed study of the embedding of the gold nanoparticles (at temperatures $T > T_{\mathrm{g}}$) than was presented previously [28]. This figure shows the average values of the apparent height for a distribution of ~ 15–20 spheres embedding as a function of time at a temperature of 378 K. Figure 3 also shows images of the samples at different stages in the embedding process. The observed (above T_{g}) embedding behaviour is qualitatively the same as that observed for micron sized silica glass spheres on plasticized PS substrates [34]. Figure 3 shows that the spheres do not become fully embedded as expected based upon the previous discussion. This is clearly demonstrated by the images shown for the 20 nm spheres. The first image shows the spheres on the PS films before heating. The final image is taken after 2630 minutes of annealing at 378 K and shows that a significant fraction
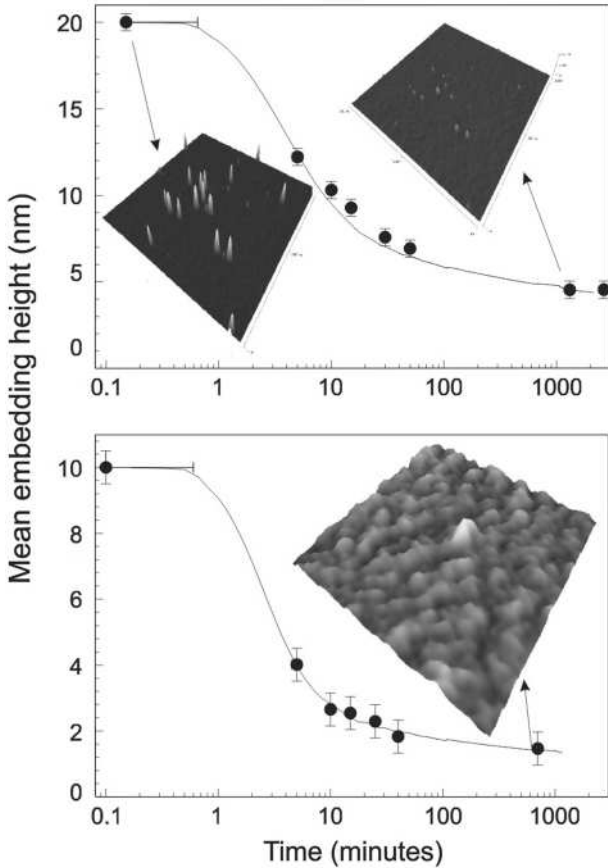
Fig. 3. Kinetics of the embedding of 20 nm (top) and 10 nm (bottom) Au spheres into PS melt at ($T = 378$ K). The images are taken at the times indicated on the figures, using scan sizes of $3\,\mu$m $\times$ $3\,\mu$m for the upper graph and $0.3\,\mu$m $\times$ $0.3\,\mu$m for the lower graph. Most of these data have been reproduced from reference [28]. The solid lines shown in these plots show the results of the simulations that are based on the theoretical model developed by Lee and Radok [38] and Lu *et al.* [39]. These simulations were performed using a simulation temperature of 379 K and by assuming equilibrium PS/Au contact angles of 46° and 59° for the 10 and 20 nm Au particles, respectively (see text).

of each sphere still remains above the surface of the films. The data in the figure also shows that the embedding of both the 10 nm and 20 nm diameter gold nanoparticles is essentially complete after 1000 minutes and so we suspect that the final values of the embedding height are equilibrium values. If the PS-Au contact angle is the driving force for the embedding process as suggested above and the colloid particles are exactly spherical, then the value $h(t)/2R$ will be the same for both sphere sizes at the final embedding height, h. This equality is not exactly obeyed for the data shown in Figure 3. The 20 nm spheres give a value of $h_\infty/2R = 0.24$, while the 10 nm spheres give a value $h_\infty/2R = 0.15$. In terms of completely spherical particles with identical surface energies, these numbers correspond to final tangential angles between the flat surface and embedded sphere of $59 \pm 3°$ and $46 \pm 2°$, respectively. A comparison with the diagrams shown in

Figure 2a) shows that these angles should both be equal to the equilibrium PS/Au contact angle. While the values for the final tangential angles are significantly different, there are reasons why we might not expect perfect agreement between the two sets of results. In such samples the surface energies will depend crucially on the detailed surface chemistry of the Au spheres. While this should be the same for a single batch of spheres, we expect that there will be variations between different sphere sizes and even different batches of the same sphere size.

The embedding of the nanoparticles into the surface of the PS samples was modelled using a previously developed theoretical framework for the embedding of spherical nanoindenters into the surface of a linear viscoelastic material [38,39]. Lu and coworkers have shown that the embedding height, $h(t)$ of a spherical nanoindenter embedding into the surface of a linear viscoelastic material, under the action of an arbitrary time-dependent loading force, $F(t)$, can be described by the following equation [39]:

$$h\left(t\right) = 2R - \left(\frac{3(1-\nu)}{8\sqrt{R}}\int_0^t J(t-\xi)\frac{\mathrm{d}F}{\mathrm{d}\xi}\mathrm{d}\xi\right)^{\frac{2}{3}}, \qquad (2)$$

where $J(t)$ and ν are the creep compliance and Poisson's ratio of the viscoelastic medium, respectively, R is the radius of curvature of the nanoindenter and t is the elapsed time. The time derivative of the force given in this equation was replaced using the substitution $\frac{\mathrm{d}F}{\mathrm{d}\xi} = \frac{\mathrm{d}F}{\mathrm{d}h}\frac{\mathrm{d}h}{\mathrm{d}\xi}$ and the embedding height dependence of the force exerted on the gold nanoparticles was used to simulate the embedding of the Au particles into the PS surface. Values of the temperature-dependent surface tension and Poisson's ratio of PS ($\nu = 0.325$) were obtained from reference [36] and the equilibrium contact angle of PS on gold used in the calculations was 46° for the 10 nm spheres and 59° for the 20 nm spheres (as determined from the data). The creep compliance was obtained from data for a 189000 $M_{\rm w}$ PS that was kindly supplied by D.J. Plazek (University of Pittsburgh) and which has been described in reference [40]. The creep compliance data was collected at a temperature of 373 K. This data was then used to calculate the creep compliance at an arbitrary embedding temperature, T, using time-temperature superposition and by shifting the creep compliance curves along the time axis by dividing the time by the WLF shift factor, a_T. The value of a_T was calculated using the expression $\log a_T = -12.35 + 383/(T - 342)$ [40,41], where a_T was determined using a reference temperature of 373 K.

The results of the simulations described above are shown as the solid lines in Figure 3. This figure clearly shows that the embedding model described above can be used to fit the embedding data for both of the sphere sizes studied at a temperature of 378 K using a simulation temperature of 379 K. This suggests that the functional form that was used to model the force applied to the particles has the correct functional dependence upon the embedding height.

The most stringent test of the functional form used for the forces acting on the particle is how well it can

be used to model the embedding behaviour of both the 10 nm and 20 nm particles. As result of the approximation $\cos(\phi) \approx (h - R)/R$, as well as differences in the compliance values used from the samples in our study (due to the difference in M_w for instance), we expect the force expression may be modified by a constant numerical factor of order unity. Upon performing the calculations we found that the embedding data for $T > T_g$ can be described very accurately if a simple multiplicative factor of 7 is introduced to the product of the terms found inside the integrand in equation (2). This factor compensates for the fact that the approximation used for $\cos(\phi)$ above underestimates the contour length of the contact line between the PS and the gold nanoparticles and hence would be expected to underestimate the size of the forces applied to the gold particles in the initial stages of embedding. We note that this factor is *independent* of the particle size and temperature, and this independence is crucial to get a universal form for the force law.

As a cautionary note, it is worth remarking at this stage that great care needs to be taken when applying the above model to the embedding of spherical particles. This is because equation (2) is only valid for a monotonically increasing contact area between the embedding particles and the viscoelastic surface [38]. The consequences of this result are that the model should not be valid for all embedding heights less than the particle radius R. However, despite this restriction on the validity of the equations presented above, the agreement between the simulations and the embedding data is rather striking and strongly suggests that the proposed model accurately describes the embedding process at temperatures above the bulk T_g of the PS.

Films with $T < T_g$

Having gained a detailed understanding of how the spheres embed into the PS melt, the embedding of the same spheres into a sample with $T < T_g$ can be investigated. Before presenting results, it is useful to consider what we might expect in the case of different possible physical properties of the PS surface. Clearly, if the surface is glassy like the rest of the film and the forces between the gold spheres and the surface are small, we would not expect to see any embedding. In the case where the surface forces are large, plastic flow may result. This case is excluded for all but the first 0.2 nm of the embedding (see Fig. 2). A final possibility is that the surface properties of the PS are *not* the same as the glassy film. In this case we would expect to see a partial embedding where the extent of embedding does not depend on the size of the particle but only on the thickness of the surface region. Figure 4 shows the embedding of 10 nm and 20 nm gold nanospheres at temperatures as low as 7 K below the bulk T_g value. It is clear from this figure that the spheres do partially embed at sub-T_g temperatures. The extent of embedding ($\sim 3.5 \pm 0.5$ nm) and timescale for embedding (50–100 minutes) are observed to be similar for both the 10 nm and 20 nm spheres. We note that the values here are similar to those
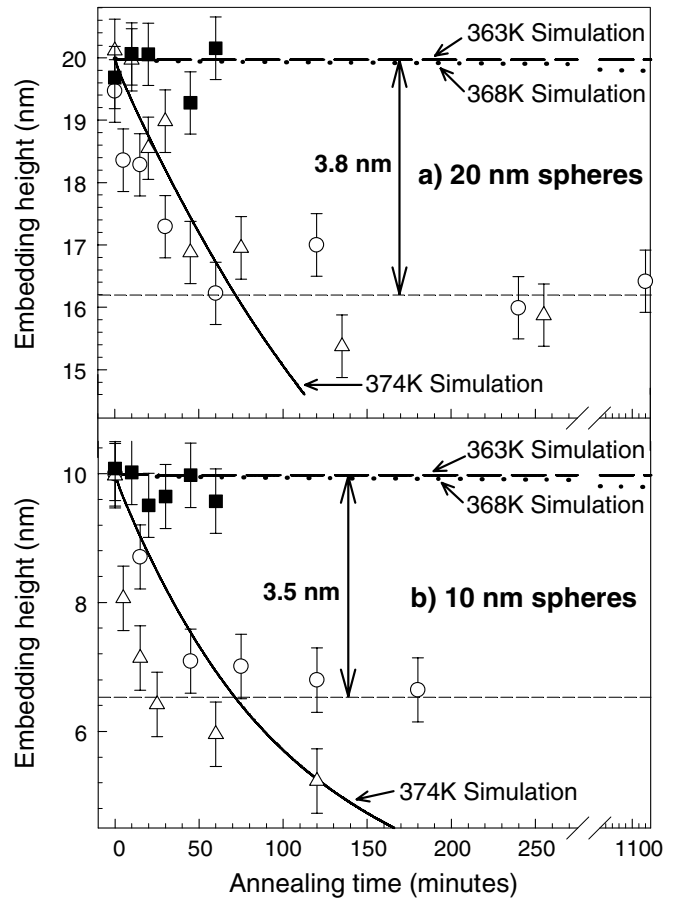
Fig. 4. Kinetics of the embedding of Au spheres into PS over a range of temperatures below the bulk T_g value. Data are shown for the embedding of Au spheres at temperatures of 363 K (○) and 368 K (△) ($T < T_g$(bulk)). Panel a) shows data for the embedding of 20 nm Au spheres into PS. Data are also shown for the change in the measured height of 20 nm Au spheres on a bare Si surface that were collected at a temperature of 363 K (■). The dashed and dotted lines shown in panel a) are the results of simulations of the embedding of 20 nm Au particles into the surface of a PS film that were performed at simulation temperatures of 363 K and 368 K, respectively (see text). The solid line shown in panel a) is the result of a simulation of the embedding of the 20 nm particles that was performed using a simulation temperature of 374 K. Panel b) shows the kinetics of embedding of 10 nm Au spheres into PS at the same temperatures used for the 20 nm spheres. Data are also shown for the change in the measured height of 10 nm Au spheres on a bare Si surface that were collected at a temperature of 363 K (■). The dashed and dotted lines shown in panel b) are the results of simulations of the embedding of 10 nm Au particles into the surface of a PS film that were performed at simulation temperatures of 363 K and 368 K, respectively. The solid line shown in panel b) is the result of a simulation of the embedding of the 10 nm particles that was done using a simulation temperature of 374 K. Most of the sub-T_g embedding data shown in this figure has been reproduced from reference [28].

of reference [29] where embedding to a depth of 4 nm was observed at temperatures as low as 313 K. Figure 4 also shows the apparent height of the Au nanospheres as a function of time on top of a bare Si substrate at a temperature $T = 363$ K. These data show that the surface properties of the spheres themselves are not changing with time at temperatures up to 363 K. Measurements of the spheres on bare Si substrates were also taken at temperatures above the T_g value to be compared with the results shown in the previous section. These showed essentially the same behaviour as the sub-T_g measurements that were performed on Si substrates. These combined data sets suggest the qualitative conclusion that at the temperatures measured, the first ~ 4 nm of the surface does not vitrify.

A more quantitative conclusion can be made by considering extensions of the simulations described in the previous section. Figure 4 shows the results of simulations of the embedding of the gold spheres in to the surface of PS at $T < T_g$. It is unreasonable to expect equilibrium wetting of the gold by a glassy PS surface to occur due to the non-equilibrium state of the PS at these temperatures. However, it is worth noting that the analytical form assumed for the magnitude of the forces in the embedding calculations used above represents a reasonable approximation to the forces that would be exerted on the particles by a glassy PS surface. The only difference being that the forces exerted on the particles would have a slightly different functional dependence upon the embedding height. The results of the simulations shown in Figure 4 illustrate that the embedding of the nanoparticles at temperatures below the bulk T_g of PS into a PS surface that has the same T_g as the bulk polymer (363 K and 368 K, shown as dashed and dotted lines, respectively) would be expected to embed by less than 0.5 nm on the timescales of the embedding experiments. This clearly deviates from the observed values, and thus the bulk compliance values at the experimental temperature *cannot* be used to explain the embedding of nanospheres at $T < T_g$. Instead, the first 3–4 nm of the embedding data for both the 10 nm and 20 nm Au particles are accurately modelled using a simulation temperature of 374 K *i.e.* this more quantitative analysis shows that the material within the first 3–4 nm of the free PS surface behaves like a polymer melt having a temperature of 374 K for experimental embedding temperatures that are at least 7 K below the bulk T_g of the polymer. This means that as one cools the polymer down below T_g, the bulk of the sample vitrifies, but the 3–4 nm near the free surface *continues to behave as if it were at a temperature, $T = 374$ K* at temperatures that are at least 7 K below the bulk T_g.

The data and the results of the simulations shown in Figure 4 strongly suggest that there is a 3–4 nm thick *liquid-like* near-surface region in glassy PS. However, it is clear that the simulations do not predict the 65 K temperature difference between the material properties of the free surface and the bulk material that could be inferred from measurements of the T_g of free standing polymer films [8]. This is because care has to be taken when interpreting the results of the studies performed on free standing polymer films. The results of the experiments performed on freely standing PS films by Forrest *et al.* [8], suggest that there is a layer at the surface of the PS films which is *liquid-like* and that the enhanced mobility in this layer persists in films that are up to 65 K below their corresponding bulk T_g. The results of the embedding simulations are consistent with these arguments if there is a layer at the surface of the films with a higher mobility, having properties similar to those of the bulk polymer at a temperature of 374 K and which remains this way until it finally "freezes" at some temperature which is at least 65 K below the bulk T_g of the polymer. The properties of the PS near the surface are also expected to be very inhomogeneous and the lengthscales associated with the size of the embedding particles are significantly larger than the lengthscales involved in the segmental level relaxations that are probed during T_g measurements. Any excess mobility at the free surface is also restricted to a region of a few nm and this will have a large influence on the flow that will be allowed and also on the dynamics of particle embedding. The polymer segments in the near-surface region are also highly likely to belong to polymer molecules that have segments in glassy parts of the film. This is expected to impose constraints on chain motion and will inevitably affect how the spheres embed. It is also expected that the above factors would further complicate the dynamics of the embedding process, so that the value of 374 K derived from the simulation results may represent an average of the properties of the liquid-like layer in the near-surface region.

The physical contact between the gold nanoparticles and the PS films used also means that the surface the particles embed into is also not strictly a "free surface". This is a concern that must be addressed in detail before any attempts to relate the results presented here to the properties of the free surface can be made. The most basic question to address is what would be observed if the surface layer has enhanced mobility and what would happen if the surface is glassy. If the surface is glassy, then the expected observations are obvious —no motion is possible and there will be no embedding of any particles for $T < T_g$. This is clearly not observed in the embedding studies presented here. It is reasonable to conclude therefore, that the *surface region immediately underneath the Au nanospheres is not glassy*. The most obvious indication that gold does not plasticize the PS is provided by the measurements of T_g on Au coated films presented below and in reference [42]. Studies performed by Faupel *et al.* [43] have also shown that polymer chain motion is slower near gold surfaces than it is in the bulk. Furthermore, studies by Cole *et al.* [44] have shown that Au filled polymer has a higher viscosity than pure polymer. It is unlikely therefore that the Au spheres are responsible for plasticising the surface of the PS films. The enhanced mobility must arise because the nanoparticles are close to the free surface of the PS films. If we consider a region underneath the nanoparticles, it is reasonable that its dynamics will be influenced by the free surface if the region can be connected to the free surface with *any* line of some length λ_{FS} that describes the lengthscale of the free surface region with enhanced

dynamics. This lengthscale can be determined by considering the onset of reduced T_g values in either free standing or supported films by noting when the properties of the whole film are influenced by the effects of the free surface. This process suggests a lengthscale, $\lambda_{FS} \sim 10$ nm [31]. The effects of the solid surface of the nanoparticles doing the embedding also need to be considered. The presence of these solid surfaces will have the effect of negating any free surface effect over some other lengthscale λ_{sub} close to the surface of the nanoparticles. A previous analysis [12] suggested that the lengthscale associated with the effects of a solid surface (or substrate) on the measured T_g was ~ 2 nm. We would expect therefore that a region near the free surface covered by the nanoparticles will have an enhanced mobility if it is within λ_{FS} of the free surface but *not* within λ_{sub} of the nanoparticle surface. These conditions are fulfilled in the present experiment. In other words, there will be a region of enhanced mobility underneath the nanoparticles that is still influenced by the free surface and will still exhibit an enhanced mobility. This modifies how the results of Figure 4 should be interpreted. The fact that the nanoparticles embed 3–4 nm means that there is a more mobile surface region with a characteristic size that has a *lower bound* of 3–4 nm.

Effect of free surfaces on T_g value in thin films

T_g in films with evaporated coatings

The thickness dependence of the T_g of thin supported films of PS with one free surface (uncapped) are shown in Figure 5a). This plot also shows $T_g(h)$ for PS films of similar thickness that have been coated with a 5 nm thick layer of gold (Au). The uncapped films show depressions in T_g as the film thickness is decreased below 40 nm with a maximum measured T_g depression of 15 K being observed for an 8 nm thick film. The T_g values obtained in this study are within the acceptable range of values obtained in other studies [31]. The T_g of the Au capped films have a significantly different thickness dependence to the uncapped films. The Au capped films are shown to have a bulk T_g of 370 ± 1 K and this value is shown to persist for all film thickness ≥ 8 nm. These results are consistent with the experiments performed on thin supported PS films [3] and freely standing films of PS [12,31] which provide strong evidence that the free surface is important in determining the T_g of thin polymer films. Coating the PS films with an evaporated metal layer in this way is expected to remove the effects of the free polymer surface and to give rise to bulk-like behaviour even for the thinnest films studied.

Figure 5b) shows the thickness dependence of the T_g in thin supported PS films that have been coated with a 5 nm thick thermally evaporated aluminium (Al) layer. The solid line in this plot also shows the best fit to the uncapped film data that was obtained by using the empirical expression $T_g(h) = T_g(\text{bulk})(1 - (\alpha/h)^\delta)$ (best fit $\alpha = 0.28$, $\delta = 0.95$) [3]. In contrast to the Au capped films, the Al capped films have a thickness dependent T_g, with depressions being observed for film thickness < 20 nm.
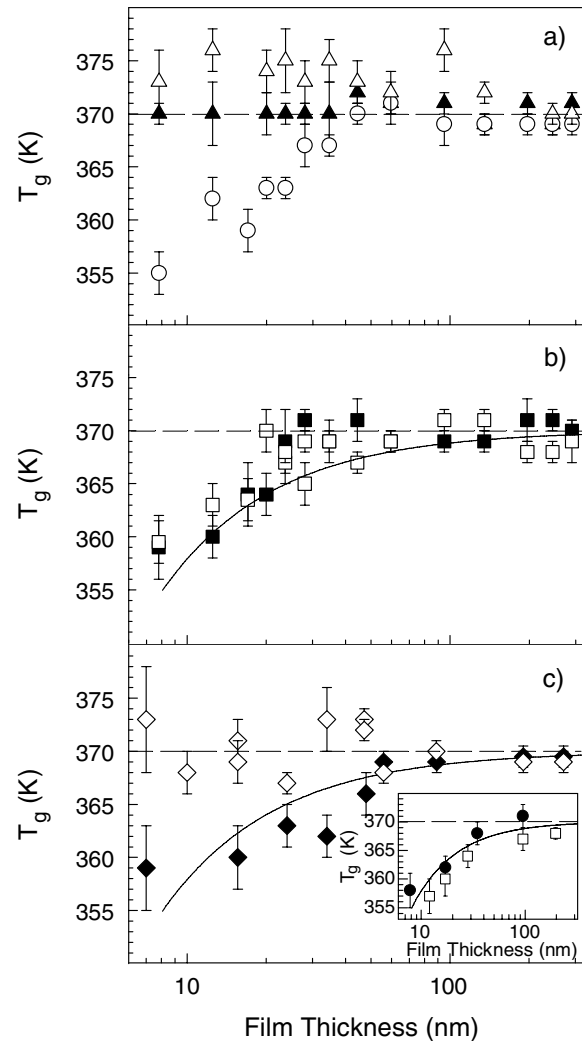
Fig. 5. Thickness dependence of the glass transition temperature (T_g) in thin polystyrene films. Panel a) shows data for uncapped spin-cast PS films supported on silicon (Si) substrates ($\circ$ from Ref. [42]) and PS films that have been capped with a 5 nm thick thermally evaporated gold (Au) layer. The two evaporating/annealing histories used are for films that have been capped then annealed ($\triangle$) and annealed then capped with Au ($\blacktriangle$ from Ref. [42]). Panel b) shows the best fit to the data for uncapped PS films (solid line) as well as data for PS films that have been capped with a 5 nm thick thermally evaporated Aluminium (Al) layer. Two different evaporating/annealing histories were used. Data are shown for films that have been capped then annealed ($\square$) and annealed then capped with Al ($\blacksquare$ from Ref. [42]). Panel c) shows the thickness dependence of the T_g in the $2(h/2)$ films. Data were collected both before ($\diamondsuit$) and after ($\blacklozenge$) dissolution of the Al layer in 1 M NaOH$_{(aq)}$. Both of these data sets have been reproduced from reference [42]. The inset shows the thickness dependence of the measured T_g for uncapped films that were immersed in saturated NaCl$_{(aq)}$ solutions for 4 hours prior to annealing ($\bullet$) and for uncapped films that were immersed in 1 M NaOH$_{(aq)}$ solutions for 5 minutes ($\square$). The solid lines represent the best fit to the data obtained for the uncapped films shown in panel a). All the data was obtained using a cooling rate of 1 K min^{-1}.

The T_{g} depressions in the Al capped films are comparable to those observed in the uncapped films (11 ± 2 K for a 8 nm thick film). As discussed above, capping the PS films with a metal layer is expected to suppress the film thickness dependence of the T_{g}. This is clearly not the case for the Al capped films studied in the present work. The behaviour reported here for Al capped films has also been observed in broadband dielectric studies of Al capped PS films that were prepared in a similar way to the samples used in the present study [26].

Characterisation of the polymer-metal interface

The observed differences in the thickness dependence of the T_{g} of Al capped and Au capped films could be explained by differences in the structure of the polymer-metal interfaces that are produced during thermal evaporation of the metal capping layers. Studies by Faupel *et al.* [43] and Strunskus *et al.* [45,46] have shown that the structure of polymer-metal interfaces is sensitive to the choice of metal and the deposition parameters used during thermal evaporation. These studies have shown that in systems where the polymer-metal interaction is relatively weak (such as gold and polyimides and gold and polycarbonates), the width of the polymer-metal interface is much broader (typically tens of nanometres) than the interface between more reactive metals like aluminium and the same polymers. The interfacial width is also shown to be broader for low evaporation rates. These effects are attributed to the fact that unreactive metals deposited at low evaporation rates do not always form the critical cluster size required to prevent significant diffusion of the metal atoms in to the polymers [46]. This allows isolated metal atoms that are not captured by a growing cluster of similar metal atoms to diffuse into the polymer films even for films that are below their bulk T_{g} [43]. The evaporation rates used in the deposition of Au in the present study are comparable to those described by Faupel *et al.* and others, in cases where significant interface formation has been observed in other polymer-metal systems. In the case of more reactive metals (such as Al) the interface between the polymer and metal has been shown to be very sharp [43,47]. This is attributed to the polymer-metal interaction which localizes the evaporated Al atoms at the polymer surface and allows formation of the critical cluster sizes required to prevent significant diffusion of the metal atoms into the polymer films. The results of the studies by Faupel *et al.* and Strunskus *et al.* suggest that the Al and Au capped films used in the present T_{g} studies may have polymer-metal interfaces with significantly different structures.

To test the hypothesis that the distribution of the evaporated metals in the polymer was different for Au and Al capping layers, AFM experiments were performed on inverted metal layers that had been evaporated on top of PS films. These samples were prepared using the procedure described in the experimental section. Figure 6 shows contact-mode AFM images taken over a $20\,\mu\mathrm{m} \times 20\,\mu\mathrm{m}$ area of both Au (Fig. 6a)) and Al (Fig. 6b)) surfaces after
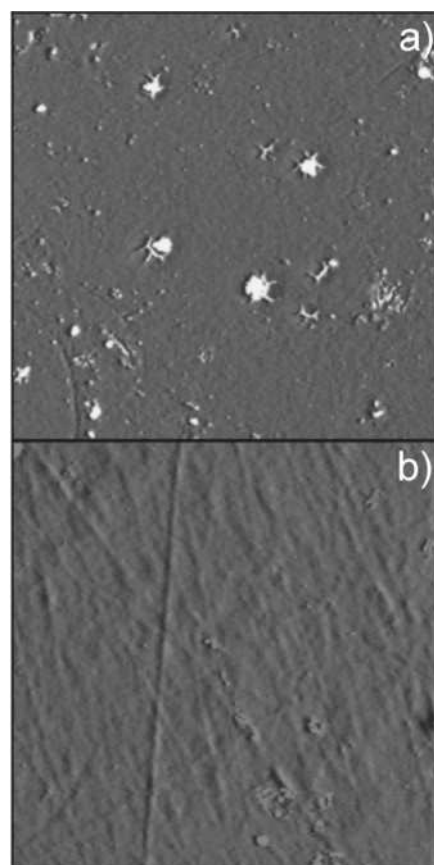
Fig. 6. Atomic force microscope (AFM) images of PS-metal interfaces after dissolution of the PS layer. Data are shown for an a) Au-PS interface and for a b) Al-PS interface for films where the PS film was annealed and the metal layer subsequently evaporated on top of the polymer film. Data were collected using contact mode AFM with a scan size of $20\,\mu\mathrm{m} \times 20\,\mu\mathrm{m}$ (height: 10 nm).

the PS film has been dissolved away. The data obtained in these images can be used to show that the Au-PS interface typically has a root mean square (r.m.s.) roughness of 4.2 nm, but also that these interfaces have a number of dense gold structures that extend up to 20 nm into the PS films. This observation is consistent with the studies performed by Faupel *et al.* [43] on other gold-polymer interfaces that also show the presence of gold clusters that extend tens of nanometres into the polymer. AFM images of the inverted Al surfaces revealed that the Al-PS interface was much sharper than that observed in the Au-PS system, typically having an r.m.s. roughness of 0.5 nm. No large clusters were observed on the inverted Al surfaces but some anisotropy was observed in the structures that were imaged. The long stringlike structures observed (Fig. 6b)) are similar to those reported by LeGoues *et al.* [47].

Whilst the images of the inverted metal surfaces collected give some indication of the types of structures present in the original polymer-metal interfaces they do not explain how the differences in interfacial structure relate to differences in the measured T_{g} values. However, the correspondence between the results obtained in the

present study and those obtained in other studies is encouraging and suggests that the structure of the polymer-metal interface may play a role in determining the thickness dependence of the T_g in metal capped films. Strunskus *et al.* [46] suggest that after evaporating, the metal capping layer and polymer film are not in perfect contact and that the mismatch in expansion coefficients of the polymer and metal capping layer can give rise to crack formation at the interface between the two materials upon heating. In the case of Al capped films such a mismatch could cause the sharp polymer-metal interface to fail and expose the polymer surface [47]. This would explain why the measured T_g's in the Al capped PS films are similar to those measured for the uncapped films. Failure of this interface could have arisen because of the heating introduced by the thermal evaporation procedure. However, both sets of Al capped films were also heated above their bulk T_g value during the ellipsometric T_g measurement and so we might expect that delamination could occur for both of the evaporation/annealing histories studied during this heating step. The broad polymer-metal interfacial width observed in the PS-Au systems is expected to have stronger adhesive properties than the sharp interface formed in the PS-Al system [43,46] and should be more resistant to this mode of failure.

In addition to the possibility of interfacial failure re-exposing the free surface, there is an additional reason why evaporating a thin coating onto a polymer film may not be adequate to remove the effects of the previously "free surface". It has been demonstrated in numerous systems that polymer chain mobility may be significantly slower near polymer/metal interfaces. As discussed above, Faupel *et al.* [43] have shown that the presence of metal atoms in polyimide and polycarbonate films leads to the slowing-down of dynamic processes in these materials. Such effects do not seem to be limited to polymer-metal interfaces. Chain mobility has also been measured near the PS/Si interface and significant decreases in chain diffusion were reported [48]. The result of this slowing-down in chain motion is that it becomes increasingly difficult to anneal out any structural perturbations that existed at the free surface before coating. A reduction in chain mobility coupled with the observed differences in the interfacial width of the polymer-metal interfaces studied, might also explain the differences obtained for the thickness dependence of the Al and Au capped films. The broader interfaces observed for the Au capped films would result in a reduced chain mobility that persisted further into the films than would be observed for the the sharp interfaces formed in the Al capped films. Decreases in chain mobility would mean that even thorough annealing may not be adequate to relax the remaining structural perturbations.

The effects of the evaporation/annealing history upon the T_g of the metal capped films have also been determined. For Al capped films, no significant differences were observed between films that had been annealed and then coated and films that have been coated, then annealed (Fig. 5b)). In contrast, the T_g of the Au capped films was shown to have some dependence upon the order of evaporation and annealing (Fig. 5a)). Films that were evaporated onto and then annealed were found to have measured T_g values that were up to 5 ± 1 K larger than films that were annealed and then coated.

T_g in films with non-evaporated coatings

The above discussion of the behaviour of the different polymer-metal interfaces is certainly interesting and somewhat compelling. However, it is difficult to determine how important delamination and annealing effects are because of the difficulties associated with determining the amount of contact at a buried interface. These difficulties mean that another method of determining the contribution of the free surfaces (if any) to the measured T_g of thin PS films must be found. To do this Al capped films were prepared in such a way as to try to remove the difficulties and uncertainties associated with evaporative deposition. This was done by preparing a series of $2(h/2)$ films as described in the experimental section. There are a number of advantages to preparing the samples in this way when compared to simple Al (evaporative) coated films. Firstly, by evaporating the Al layer onto a NaCl substrate and then spin coating the PS film on top we ensure that the polymer-metal interface is sharp and that there are no metal atoms in the PS. Secondly, this method of sample preparation ensures that the top surface of the $2(h/2)$ samples has been in intimate contact with the capping layer during the spin coating process and removes any density defect at this top interface. In preparing the samples in such a way that their free surfaces are near the centre of the film, it is also possible to anneal away any density defects that could be responsible for the reduced T_g in thin PS films. The choice of annealing conditions used in the present study was expected to cause an increase in the width of the PS-PS interface (produced by placing the two films in contact) of between 5 and 8 nm [49–51]. This is comparable to the estimated thickness of the proposed surface layer obtained from the embedding experiments described above and in a study by Kawana *et al.* [30]. Annealing the films should therefore result in bulk properties at the centre of the films.

Figure 5c) shows the thickness-dependent T_g data for the $2(h/2)$ films and shows that there are *no significant changes in the measured T_g as the film thickness is decreased*, for films as thin as 7 nm. These results show that by placing two films in contact in this way it is possible to remove the memory of the free surfaces and suppress the film thickness dependence of the T_g in Al capped films. To illustrate that the NaCl is not responsible for suppressing the thickness dependence of the T_g, measurements were performed on uncapped PS films that had been immersed in saturated NaCl solutions for 4 hours (Fig. 5c) inset). For all the film thickness studied, the measured T_g's were the same as those measured for the uncapped PS films of the same thickness. Another equally important point about the data for the $2(h/2)$ films is that it can be used to address some of the issues often discussed concerning the origin of T_g reductions in thin PS films. Thin polymer films

have a rather tortuous sample preparation history and are certainly not in equilibrium. Vitrification upon solvent removal followed by continuing solvent evaporation results in significant in-plane stress as well as a lower density than bulk samples. Even though the samples are often annealed tens of degrees above their bulk T_g for many hours [3,12,31], it is not clear that such annealing is sufficient to remove these effects. It has been suggested that the observed T_g reductions could arise as a result of this preparation history. These concerns are addressed by the measurements performed on the $2(h/2)$ films. In making the $2(h/2)$ films the intermediate stage involves two samples of thickness $h/2$. It is clear from Figure 5a), that for $h < 40$ nm each of the $h/2$ films has a reduced T_g value. If this reduced T_g value were due to sample formation history, then the formation and subsequent annealing of the $2(h/2)$ composite sample would not remove the preparation history any more than annealing the single $h/2$ sample would. The fact that preparing the $2(h/2)$ sample eliminates the T_g reductions provides strong evidence against the idea that the specific process of spincasting the film out of a solvent causes the observed T_g reductions.

The surface can be manipulated further by the removal of the Al capping layer. Based on the arguments presented above, it is expected that this will result in the restoration of a film thickness-dependent T_g value. In fact, we would expect the films to have a T_g value typical of that of simple uncapped PS films. Figure 5c) also shows the measured T_g values for the $2(h/2)$ films *after* removal of the Al capping layer (by immersion in 1 M NaOH). The resulting samples show a film thickness-dependent T_g value. In fact the T_g value of an uncapped PS film is the same whether or not the film was prepared as a single film of thickness h, or was prepared as a $2(h/2)$ capped film and then had the capping layer removed. This process provides a method for the complete manipulation of the surface of polymer films and results in direct evidence for the effects of the free surface on the T_g value. To confirm that the NaOH treatment is not reponsible for the reductions in the measured T_g of the $2(h/2)$ films, uncapped PS films were immersed in 1 M NaOH for 5 minutes. These samples were then rinsed with deionised water and the T_g of the films measured. The inset of Figure 5c) shows data for the measured T_g values of uncapped films with thickness in the range 12–200 nm after treament with $\mathrm{NaOH_{(aq)}}$. These data show that the measured T_g values of the treated films are the same as those of untreated, uncapped films (within the limits of experimental uncertainty). This illustrates that the NaOH does not plasticise the PS films and that is not responsible for causing the reductions in T_g that are observed when the Al layer is removed from the $2(h/2)$ films. This adds further support to the idea that restoration of the free surface is responsible for the recovery of the thickness-dependent T_g in these samples.

Kawana *et al.* have also shown that as the thickness of uncapped PS films decreases, the expansion coefficient of the glass increases and tends towards that of the melt [30]. This was attributed to the glassy expansion coefficient being an average of the expansion coefficients of the bulk
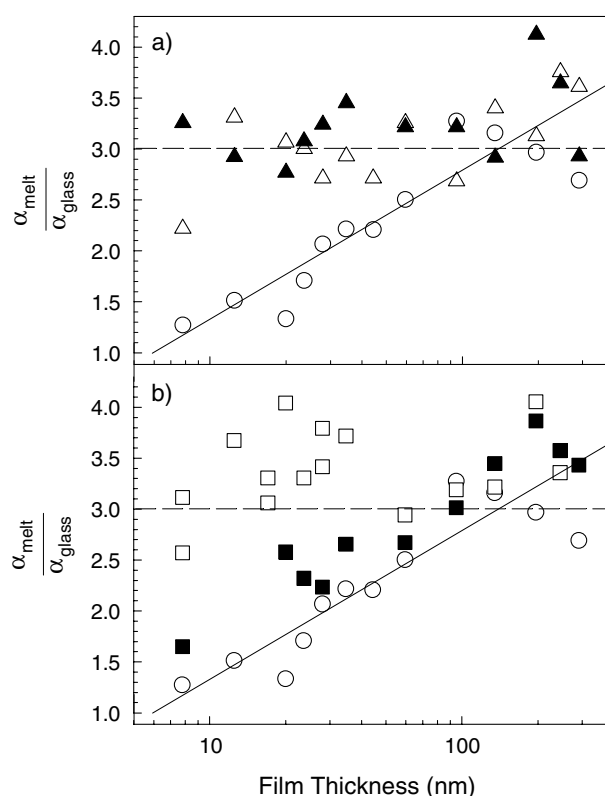
Fig. 7. Thickness dependence of the ratio of the melt and glassy expansion coefficients. Panel a) shows data for uncapped PS films ($\circ$), for films that have been capped with Au and annealed ($\triangle$) and for films that have been annealed and then capped with Au ($\blacktriangle$). Panel b) shows data for uncapped PS films ($\circ$), for films that have been capped with Al and annealed ($\square$) and for films that have been annealed and then capped with Al ($\blacksquare$).

glass and the proposed "liquid-like" layer at the surface of the glassy polymer films. The contribution of the liquid-like layer to the expansion properties of the thin glassy PS films is expected to become more important as the film thickness decreases [30]. As a result of this, the ratio of the melt and glassy expansion coefficient decreases from the bulk value to a value approaching one as the thickness of the PS films is decreased below 40 nm. This decrease in transition contrast is evident in many studies of thin film T_g values [31]. By definition, it is impossible to determine the T_g of the PS films when this ratio is equal to one, but it is possible to extrapolate the thickness-dependent behaviour of this ratio to a value of unity. This procedure provides an estimate of the thickness of the liquid-like layer [30]. Figure 7 shows the thickness dependence of the ratio of the melt and glassy expansion coefficients obtained from the ratio of the slopes taken from the P and A data obtained in the present study (Fig. 1). This figure shows that as the film thickness decreases the ratio $\alpha_{\mathrm{melt}}/\alpha_{\mathrm{glass}}$ for uncapped PS films also decreases in agreement with many other studies [31]. Extrapolating the value of the expansion coefficient ratio to one gives a value of the thickness of the liquid-like layer to be 5 ± 1 nm (Fig. 7a)). This
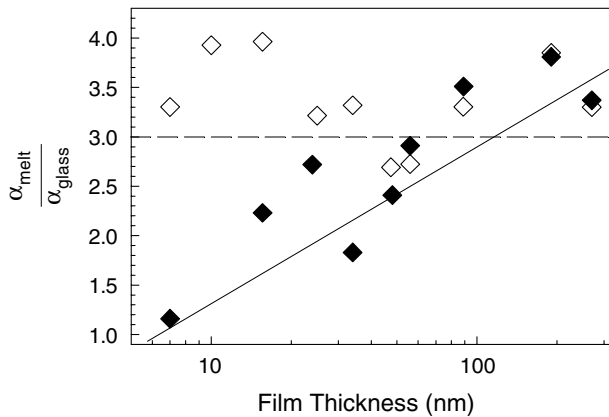
Fig. 8. Thickness dependence of the ratio of the melt and glassy expansion coefficients for the $2(h/2)$ PS films. Data were collected for $2(h/2)$ films, both before ($\diamond$) and after ($\blacklozenge$) dissolution of the Al layer in 1 M NaOH$_{(aq)}$. The solid line represents the "best fit" to the values of the ratio of the melt and glassy expansion coefficients that were obtained for uncapped PS films.

is comparable to, but smaller than, the value of 10 nm reported by Kawana *et al.*. More significantly, the value extracted from the ellipsometry data is found to be in excellent agreement with the predicted lower bound for the surface layer of 3–4 nm obtained in the embedding studies discussed above. Figure 7a) also shows the thickness dependence of the ratio $\alpha_{melt}/\alpha_{glass}$ for the Au capped films. These data show that the Au capped PS films have a ratio of $\alpha_{melt}/\alpha_{glass}$ that remains bulk-like for all film thickness ≥ 8 nm and which is also independent of the evaporating/annealing history. This behaviour is consistent with that observed for the thickness dependence of the T_g in these samples. In fact for the Au coated samples, all measured properties for films with thicknesses as small as 8 nm show behaviour that is indistinguishable from bulk PS. Figure 7b) shows the thickness dependence of the contrast ratio for the Al capped PS films. These data show that in the case where the PS films were capped with Al and annealed, the films display apparently bulk like behaviour. This is in contrast to the thickness dependence of the T_g determined from the same samples. Films that are annealed and then coated with Al display a thickness dependence of the ratio of the expansion coefficients that is essentially the same as that observed for the uncapped PS films. The results obtained for the Al capped films that are coated and then annealed is puzzling and may be an artefact of the complicated sample preparation history that results from evaporating on top of unannealed samples. Figure 8 shows the thickness dependence of $\alpha_{melt}/\alpha_{glass}$ for the $2(h/2)$ films both before and after the removal of the Al capping with NaOH. This data shows that before the Al layer is removed, this ratio is independent of the $2(h/2)$ film thickness and displays the bulk value for all film thickness ≥ 7 nm. In a manner similar to Au coated films, the $2(h/2)$ films behave like bulk PS in all measured quantities. After the Al layer was removed the measured contrast ratio of the same films displayed a thickness de-

pendence that was consistent with the measured values obtained from simple uncapped PS films.

The studies reported above show that it is the presence of the free surface that gives rise to anomalous properties in thin PS films. It is remarkable that for both the Au coated PS films as well as the Al coated $2(h/2)$ films, every measured property that was determined from the results of the ellipsometry studies suggests behaviour that is characteristic of bulk PS. This is true for films as thin as 7 nm, where simple supported films display significant anomalies in their glass transition temperatures, and glass transition strength. This provides very strong evidence for the direct role of the free surface in causing reduced T_g values in thin films of PS.

Conclusions

We have presented a detailed study of the properties of the free surface of polymer films and the effects that they have on the measured T_g value. The free surface properties were determined by looking at the embedding of nanoparticles into the polymer surface. Embedding into the PS melt has been shown to be driven by surface tension forces acting at the contact line between the PS and the Au nanoparticles. Simulations of the embedding behaviour based upon a previously developed model for the indentation of nanoscale spheres showed that surface tension could be used to accurately describe the embedding behaviour of the nanoparticles at temperatures above the bulk T_g of the PS. Extension of this analysis to glassy films revealed evidence for a liquid layer with a thickness of 3–4 nm that exists at the surface and which has properties that are similar to a bulk sample having a temperature of 374 K. An accompanying study describes the effects that thermally evaporating a thin metal capping layer has upon the glass transition temperature of thin spin-cast polystyrene (PS) films supported on silicon substrates. The T_g of uncapped films is shown to decrease for film thickness < 40 nm, with a maximum T_g depression of 15 ± 1 K being observed for an 8 nm thick film. The effects of evaporating a metal capping layer on top of the PS films is shown to depend upon the choice of metal used. Films that have been coated with a 5 nm thick gold (Au) capping layer are shown to display no T_g depressions as the thickness of the PS films is decreased for films ≥ 8 nm. Thin PS films capped with a 5 nm thick Al layer are shown to display T_g depressions similar to those observed in uncapped films. The differences in behaviour of the Al capped and Au capped films are explained in terms of the structure of the polymer-metal interfaces produced during thermal evaporation of the metal layers. Measurements were also performed on samples where the capping layer was applied without using thermal evaporation. These samples had identical geometries to the Al capped PS films where the Al layer was thermally evaporated on top of the polymer, except that a different sample preparation procedure was adopted. In contrast to the evaporatively Al capped films, these samples have a T_g that is independent of the film thickness for the range of film thicknesses studied

(7–270 nm). Dissolution of the metal coating results in a restoration of film thickness-dependent T_g reductions. These experiments provide strong evidence that when the effects of the free surface are removed, bulk-like behaviour is recovered in all measured quantities. This is evident from the thickness dependences of the measured T_g values and the thickness dependences of the ratio of the melt and glassy expansion coefficients. This complimentary set of studies strongly supports the existence of enhanced surface dynamics in the polymer, when the bulk is in the *glassy phase* and also that the free surface has a strong influence on the measured properties of thin polymer films.

References

1. Eur. Phys. J. E **8**, (2002).
2. J.A. Forrest, Eur. Phys. J. E **8**, 261 (2002).
3. J.L. Keddie, R.A.L. Jones, R.A. Cory, Europhys. Lett. **27**, 59 (1994).
4. J.L. Keddie, R.A.L. Jones, R.A. Cory, Faraday Discuss. Chem. Soc. **98**, 219 (1994).
5. L. Hartmann, J. Gorbatschow, J. Hauwede, F. Kremer, Eur. Phys. J. E **8**, 145 (2002).
6. J.S. Sharp, J.A. Forrest, Phys. Rev. E **67**, 031805 (2003).
7. Y. Grohens, L. Hamon, G. Reiter, A. Soldera, Y. Holl, Eur. Phys. J. E **8**, 217 (2002).
8. J.A. Forrest, K. Dalnoki-Veress, J.R. Stevens, J.R. Dutcher, Phys. Rev. Lett. **77**, 2002 (1996).
9. J.A. Forrest, K. Dalnoki-Veress, J.R. Dutcher, Phys. Rev. E **56**, 5705 (1997).
10. K. Dalnoki-Veress, J.A. Forrest, C. Murray, C. Gigault, J.R. Dutcher, Phys. Rev. E **63**, 031801 (2001).
11. P.G. deGennes, Eur. Phys. J. E. **2**, 201 (2000).
12. J.A. Forrest, J. Mattsson, Phys. Rev. E. **61**, R53 (2000).
13. J. Mattsson, J.A. Forrest, L Borjesson, Phys. Rev. E **62**, 5187 (2000).
14. S. Herminghaus, K. Jacobs, R. Seeman, Eur. Phys. J. E. **5**, 531 (2001).
15. D. Long, F. Lequeux, Eur. Phys. J. E **4**, 371, (2001).
16. K.L. Ngai, J. Phys. IV **10**, Pr7-221 (2000).
17. J. Hammerschmidt, W. Gladfelter, G. Haugstad, Macromolecules **32**, 3360 (1999).
18. S. Ge, Y. Pu, W. Zhang, M. Rafailovich, J. Sokolov, C. Buenviaje, R. Buckmaster, R.M. Overney, Phys. Rev. Lett. **85**, 2340 (2000).
19. Z. Fakhraai, J. Forrest, unpublished.
20. M. Hamdorf, D. Johannsmann, J. Chem. Phys. **112**, 4262 (2000).
21. T. Kerle, Z.Q. Lin, H.C. Kim, T.P. Russell, Macromolecules **34**, 3484 (2001).
22. H. Fischer, Macromolecules **35**, 3592 (2002).
23. H. van Melick, A. van Dijken, J. den Toonder, L. Govaert, H. Meijer, Philos. Mag. A **82**, 2093 (2002).
24. J.A. Forrest, J. Mattsson, L. Borgesson, Eur. Phys. J. E **8**, 129 (2002).
25. V. Zaporojtchenko, T. Strunskus, J. Erichsen, F. Faupel, Macromolecules **34**, 1125 (2001).
26. K. Fukao, S. Uno, Y. Miyamoto, A. Hoshino, H. Miyaji, Phys. Rev. E **64**, 051807 (2001).
27. J.H. Teichroeb, J.A. Forrest, Proc. Symp. Mat. Res. Soc. **734**, B3.2.1 (2001).
28. J.H. Teichroeb, J.A. Forrest, Phys. Rev. Lett. **91**, 016104 (2003).
29. V.M. Rudoy *et al.*, Colloid J. **64**, 746 (2002).
30. S. Kawana, R.A.L. Jones, Phys. Rev. E. **63**, 021501 (2001).
31. J.A. Forrest, K. Dalnoki-Veress, Adv. Colloid Interface Sci. **94**, 167 (2001).
32. D.R. Lide (Editor), *CRC: Handbook of Chemistry and Physics*, 74th edition (CRC Press, London, 1993-1994).
33. H. Kim, A. Rhm, L.B. Lurio, J.K. Basu, J. Lal, D. Lumma, S.G. J. Mochrie, S.K. Sinha, Phys. Rev. Lett. **90**, 068302 (2003).
34. D.S. Rimai, D.M. Schaefer, R.C. Bowen, D.J. Quesnel, Langmuir **18**, 4592 (2002).
35. F.M. Orr, L.E. Scriven, A.P. Rivas, J. Fluid Mech. **67**, 723 (1975).
36. J. Brandrup, E.H. Immergut, E.A. Grulke (Editors), *Polymer Handbook*, 4th edition (Wiley-Interscience, New Jersey, 1999).
37. B. Du, O.K.C. Tsui, Q. Zhang, T. He, Langmuir **17**, 3286 (2001).
38. E.H. Lee, J.R.M. Radok, J. Appl. Mech. **27**, 438 (1960).
39. H. Lu, B. Wang, J. Ma, G. Huang, H. Viswanathan, Mech. Time-Dependent Mater. **7**, 189 (2003).
40. D.J. Plazek, V.M. O'Rourke, J. Polym. Sci. A-2 **9**, 209 (1971).
41. D.J. Plazek, private communication.
42. J.S. Sharp, J.A.Forrest, Phys. Rev. Lett. **91**, 235701 (2003).
43. F. Faupel, R. Willecke, A. Thran, Mater. Sci. Eng. Rep. **22**, 1 (1998).
44. D.H. Cole, K.R. Shull, P. Baldo, L. Rehn, Macromolecules **32**, 771 (1999).
45. T. Strunskus, M. Keine, R. Willecke, A. Thran, C.V. Bechtolsheim, F. Faupel. Mater. Corr. **49**, 180 (1998).
46. T. Strunskus, V. Zaporojtchenko, K. Behnke, C.V. Bechtolsheim, F. Faupel., Adv. Eng. Mater. **22**, 489 (2000).
47. F.K. LeGoues, B.D. Silverman, P.S. Ho, J. Vac. Sci. Technol. A **6**, 2200 (1988).
48. X. Zheng *et al.*, Phys. Rev. Lett. **79**, 241 (1997).
49. G. Reiter, U. Steiner, J. Phys. II **1**, 659 (1991).
50. T.P. Russell, A. Karim, A. Mansour, G.P. Felcher, Macromolecules **21**, 1890 (1988).
51. A. Karim, G.P. Felcher, T.P. Russell, Macromolecules **27**, 6973 (1994).